



## Discover Generics

Cost-Effective CT & MRI Contrast Agents



WATCH VIDEO

# AJNR




## **The Influence of Nonaerated Paranasal Sinuses on DTI Parameters of the Brain in 6- to 9-Year-Old Children**

Marjolein H.G. Dremmen, Dorottya Papp, Juan A. Hernandez-Tamames, Meike W. Vernooij and Tonya White

This information is current as of June 16, 2025.

*AJNR Am J Neuroradiol* published online 2 November 2023  
<http://www.ajnr.org/content/early/2023/11/02/ajnr.A8033>

# The Influence of Nonaerated Paranasal Sinuses on DTI Parameters of the Brain in 6- to 9-Year-Old Children

 Marjolein H.G. Dremmen, Dorottya Papp,  Juan A. Hernandez-Tamames,  Meike W. Vernooij, and  Tonya White



## ABSTRACT

**BACKGROUND AND PURPOSE:** DTI is prone to susceptibility artifacts. Air in the paranasal sinuses can cause field inhomogeneity, thus affecting measurements. Children often have mucus in their sinuses or no pneumatization of them. This study investigated the influence of lack of air in the paranasal sinuses on measurements of WM diffusion characteristics.

**MATERIALS AND METHODS:** The study was embedded in the Generation R Study, a prospective population-based birth cohort in Rotterdam (the Netherlands). Brain MR imaging studies (1070 children, 6–9 years of age) were evaluated for mucosal thickening of the paranasal sinuses. Nonaeration of the paranasal sinuses (modified Lund-Mackay score) was compared with that in a randomly selected control group. The relationship between nonaerated paranasal sinuses and fractional anisotropy and mean diffusivity in the DTI fiber tracts was evaluated using ANCOVA and independent *t* tests.

**RESULTS:** The prevalence of mucosal thickening was 10.2% (109/1070). The mean modified Lund-Mackay score was 6.87 (SD, 3.76). In 52.3% (57/109),  $\geq 1$  paranasal sinus was not pneumatized. The results are reported in effect sizes (Cohen's *d*). Lower mean fractional anisotropy values were found in the uncinate fasciculus (right uncinate fasciculus/right frontal sinus,  $d = -0.60$ ), superior longitudinal fasciculus (right superior longitudinal fasciculus/right ethmoid sinus,  $d = -0.56$ ; right superior longitudinal fasciculus/right sphenoid sinus,  $d = -2.09$ ), and cingulate bundle (right cingulum bundle/right sphenoid sinus,  $d = -1.28$ ; left cingulum bundle/left sphenoid sinus,  $d = -1.49$ ). Higher mean diffusivity values were found in the forceps major/right and left sphenoid sinuses,  $d = 0.78$ .

**CONCLUSIONS:** Nonaeration of the paranasal sinuses is a common incidental finding on pediatric MR imaging brain scans. The amount of air in the paranasal sinuses can influence fractional anisotropy and, to a lesser degree, mean diffusivity values of WM tracts and should be considered in DTI studies in pediatric populations.

**ABBREVIATIONS:** CGB = cingulum bundle; FA = fractional anisotropy; FDR = false discovery rate; Fma = forceps major; ILF = inferior longitudinal fasciculus; IQ = intelligence quotient; MD = mean diffusivity; SLF = superior longitudinal fasciculus; UF = uncinate fasciculus; VBA = voxel-based analysis

The use of DTI to study WM microstructural development and degeneration has shown an exponential increase during the past decade. In pediatric research, DTI serves as a promising


tool for monitoring brain maturation and development from fetal life onward, and multiple studies have demonstrated age-related differences or changes in WM microstructure.<sup>1–4</sup> A disadvantage of echo-planar DTI sequences, however, is susceptibility artifacts resulting from field inhomogeneities of the static magnetic field, for example, at air/tissue or air/bone interfaces.<sup>5</sup> These inhomogeneities result in geometric distortion and signal loss, which can distort DTI measurements in the vicinity of these areas. To a certain degree, field map imaging can compensate for these artifacts, however; but it cannot completely remove the geometric distortion, and areas of complete signal loss cannot be restored.<sup>6</sup>

Received June 9, 2023; accepted after revision September 20.

From the Departments of Radiology and Nuclear Medicine (M.H.G.D., D.P., J.A.H.-T., M.W.V., T.W.) and Epidemiology (M.W.V.), Erasmus University Medical Center, Rotterdam, the Netherlands; The Generation R Study Group (M.H.G.D.), and Department of Child and Adolescent Psychiatry (T.W.), Erasmus Medical Center Sophia, Rotterdam, the Netherlands; and Section on Social and Cognitive Developmental Neuroscience (T.W.), National Institute of Mental Health, Bethesda, Maryland.

This study is financially supported through Netherlands Organization for Health Research and Development TOP project number 91211021. The general design of Generation R Study is made possible by financial support from the Erasmus Medical Center, Rotterdam; the Erasmus University Rotterdam; the Netherlands Organization for Health Research and Development; the Netherlands Organization for Scientific Research; and the Ministry of Health, Welfare and Sport. Furthermore, this study is part of the BRain development, Imaging trajectories and Deviations in brain morphology in the pEdiatric population (BRIDGE), BRIDGing the gap study. The BRIDGE gap study is made possible through financial support of an internal Erasmus Medical Center grant and of the Department of Radiology and Nuclear Medicine, Erasmus University Medical Center, Rotterdam, the Netherlands.

Please address correspondence to Marjolein Dremmen, MD, Erasmus MC Sophia, Department of Radiology and Nuclear Medicine, Room Sb-1654, PO Box 2060, 3000 CB Rotterdam, the Netherlands; e-mail: m.dremmen@erasmusmc.nl

 Indicates open access to non-subscribers at [www.ajnr.org](http://www.ajnr.org)

 Indicates article with online supplemental data.

<http://dx.doi.org/10.3174/ajnr.A8033>

## Demographic characteristics of the sample

	Total Group ( <i>n</i> = 208) (100%)	Controls ( <i>n</i> = 105) (50.5%)	Nonaerated Sinuses ( <i>n</i> = 103) (49.5%)	<i>P</i> Value
Age (mean) (SD) (yr)	8.00 (1.00)	8.17 (1.01)	7.83 (0.97)	.02
Sex (%)				.78
Male	51.9	50.5	53.4	
Female	48.1	49.5	46.6	
Ethnicity (%) <sup>a</sup>				.37
Dutch	65.9	65.7	66.0	
Other Western	8.2	9.5	6.8	
Non-Western	22.1	19.0	25.2	
Nonverbal IQ (mean) (SD) <sup>b</sup>	102.81 (14.42)	103.87 (15.72)	101.78 (13.04)	.33
Maternal education (%) <sup>c</sup>				.19
Low	4.8	1.9	7.8	
Medium	36.1	34.3	37.9	
High	46.2	50.4	41.7	
Handedness (%) <sup>d</sup>				.45
Right	87.5	89.5	85.4	
Left	9.6	7.6	11.7	

<sup>a</sup>Missing data on ethnicity (3.8%).

<sup>b</sup>Missing data on nonverbal IQ (13.0%).

<sup>c</sup>Low indicates primary school/lower vocational education; Medium, intermediate vocational education; High, higher vocational education/university. Missing data on maternal education (11.5%).

<sup>d</sup>Missing data on handedness (2.9%).

The paranasal sinuses are in close approximation to anterior-inferior brain areas, and their air content may thus influence diffusion measurements in these areas. The presence of mucus or mucosal thickening is relatively high in children compared with the adult population, peaking between 3 and 8 years of age,<sup>7,8</sup> and it is a common incidental finding on MR imaging in pediatric populations.<sup>9</sup> Reported frequencies vary due to differences in the study design and the mean age of the populations studied and range from 12% to 48%.<sup>7,10,11</sup> Furthermore, the paranasal sinuses are still developing in children, resulting in different degrees of pneumatization of the paranasal sinuses during the first 2 decades of life.<sup>12,13</sup>

WM microstructure continues to change with time in typically developing children and adolescents, with greater change in the frontal regions for all DTI parameters.<sup>14,15</sup> In addition, nonlinear trajectories have been reported with a deceleration of age-related changes in specific WM tracts in children between 4 and 11 years of age.<sup>14</sup> Thus, there is a need to evaluate the possible effect of the degree of aeration of the paranasal sinuses on DTI parameters.

In this study, we used data from a large population-based study of child development to study the influence of the degree of aeration of the paranasal sinuses on DTI parameters in the pediatric brain.

## MATERIALS AND METHODS

### Participants

The current study was embedded in the longitudinal population-based Generation R Study. An overview of the Generation R Study design is published elsewhere.<sup>16,17</sup> Briefly, the Generation R Study is a prospective birth cohort study initiated in Rotterdam between 2002 and 2006. After we obtained informed consent, a total of 9778 pregnant women or women who had recently delivered were included in the study. Demographic characteristics included age, sex, ethnicity, and educational level of the mother (Table).<sup>17</sup> In addition, the intelligence quotient (IQ) of the child was measured using the Snijders-Oomen Nonverbal Intelligence

Test 2.5–7-Revised;<sup>18</sup> and handedness, using the Edinburgh Handedness Inventory.<sup>19</sup> A neuroimaging substudy of 6- to 9-year-old children was initiated in 2009 and involved a total of 1070 children.<sup>20</sup> Exclusion criteria were general contraindications for MR imaging examination (ie, pacemaker), neurologic disorders, and claustrophobia. Informed consent was obtained from the parents before participation, and the study was approved by the Medical Ethics Committee at the Erasmus Medical Center.<sup>20</sup>

### MR Imaging Acquisition

Children were familiarized with the MR imaging scanners using a mock scanning procedure.<sup>20</sup> MR images were acquired on a 3T scanner (Discovery MR750; GE Healthcare) using an 8-channel head coil. DTI data were

obtained with 3 *b*=0 volumes and 35 diffusion directions using an EPI sequence (TR = 11s, TE = 84 ms, section thickness = 2 mm, FOV = 256 × 256 mm, *b*=1000s/mm<sup>2</sup>). The EPI phase-encoding direction was anterior-posterior. No EPI with reversed phase-encoding directions or gradient-echo field maps was acquired. In addition, an axial proton density sequence (TR = 13,500 ms, TE = 6.7 ms, section thickness = 1.0 mm, FOV = 256 × 256 mm) and a high-resolution 3D T1-weighted inversion recovery fast-spoiled gradient recalled sequence (TR = 10.3 ms, TE = 4.2 ms, section thickness = 0.9 mm, FOV = 512 × 512 mm) were obtained.

### Paranasal Sinus Assessment

The paranasal sinuses were assessed in a standardized approach by a neuroradiologist blinded to subject information. The rater evaluated whether the neuroimaging scans (*n* = 1070) showed evidence of mucosal thickening in any sinus. Subsequently, the degree of mucosal thickening of the paranasal sinuses (*n* = 109) was scored by an experienced pediatric neuroradiologist according to a modified Lund-Mackay score (Online Supplemental Data). The Lund-Mackay score is used for radiologic staging of rhinosinusitis.<sup>21–23</sup> Each sinus was assigned a score of 0 (normal aeration), 1 (partial nonaeration), or 2 (complete nonaeration). The modification of the score consisted of not assessing the maxillary sinus (due to its distance from the anterior-inferior brain regions and no expectation of it causing relevant susceptibility artifacts) and not assessing the ostiomeatal complex (which is not relevant to our study). A nonpneumatized paranasal sinus received a separate score of 3 in the modified Lund-Mackay score. The Lund-Mackay score was originally designed for CT staging, but previous studies have shown that Lund-Mackay staging of sinus disease by MR imaging is closely correlated to corresponding staging based on CT.<sup>22,23</sup>

A control group (*n* = 110) without any signs of mucosal thickening of the paranasal sinuses and with pneumatization of all sinuses (modified Lund-Mackay score of 0) was randomly

selected from an age-matched group of 6- to 9-year-old children from the same source population. After excluding DTI scans of insufficient quality for image analysis, the subset of children with nonaeration of  $\geq 1$  paranasal sinus consisted of 89 children, and the control group was 85 children. To assure an adequate sample size and because the maximum effect of nonaerated sinuses on DTI measures of the adjacent brain was hypothesized to occur in sinuses without any amount of air (so without susceptibility artifacts), we clustered the 4 groups into 2 contrasting groups: a nonaerated group with complete filling by mucosal thickening and/or no pneumatization of paranasal sinuses (score 2/3) and a control group consisting of children with normal aeration and/or partial filling by mucosal thickening (score 0/1) of the paranasal sinuses. For more detail see the flow chart in the Online Supplemental Data.

### DTI Analysis

Images were preprocessed the FMRIB Software Library, Version 6.0.2 (FSL; <http://www.fmrib.ox.ac.uk/fsl>).<sup>24</sup> Nonbrain tissue was removed, and correction for eddy current-induced artifacts and volume realignment was applied.<sup>25</sup> A weighted least-squares method was used to fit the diffusion tensor at each voxel. Probabilistic fiber tractography was run by leveraging the FSL plugin AutoPtx (<https://fsl.fmrib.ox.ac.uk/fsl/fslwiki/AutoPtx>), including the uncinate fasciculus (UF), superior and inferior longitudinal fasciculus (SLF/ILF), forceps major (FMa) and minor, cingulum bundle (CGB), and the corticospinal tract.<sup>26,27</sup> Target and exclusion masks were defined by using atlases and transferred to subject native space using nonlinear registrations obtained with FNIRT (<https://fsl.fmrib.ox.ac.uk/fsl/fslwiki/FNIRT>).<sup>28</sup> Normalization of connectivity distributions was based on successful seed-to-target attempts. Voxels unlikely to be part of the true distribution were removed by thresholding.<sup>28</sup> Average values for fractional anisotropy (FA) and mean diffusivity (MD) of each WM tract were obtained after weighting voxels on the basis of connectivity distributions. For bilateral tracts, left and right hemisphere values were averaged. To obtain global connectivity measures, we averaged all FA or MD values across the commonly used tracts and weighted this average on the basis of the volume of each tract.<sup>29</sup>

For the analysis, we focused primarily on mean FA and MD values of the WM tracts, because FA and MD values are the most widely used DTI parameters in pediatric brain imaging studies.<sup>1,4,30</sup> In addition, we developed and applied a voxel-based analysis (VBA) to study the effect of paranasal sinus content on DTI parameters in greater detail. The VBA was performed following nonlinear registration of FA maps to a study-specific EPI template in standard space.<sup>31</sup> Subsequently, an FA mask was created in standard space defined by  $FA > 0.1$  of the mean FA image. A voxelwise linear regression was performed in Python, Version 3.8.2, for each voxel within the FA mask to visualize the global effect of paranasal sinus content on FA values of adjacent WM tracts. To correct for multiple testing, we applied the Benjamini-Hochberg false discovery rate (FDR) correction, using all individual voxels within the FA mask.<sup>32</sup>

The image quality of the DTI data set was assessed using both manual and automated approaches. The manual approach included visual inspection to assess the presence of major artifacts and to assess the sum-of-squares error of tensor calculation and tract reconstructions. We also applied automatic quality control to

assess the number of slices and volumes with signal drop-out, and we excluded data with excessive motion based on translation and rotation motion parameters.<sup>29</sup> These procedures resulted in 5.0% ( $n = 11$ ) of the scans being rated as of insufficient quality, and those scans were excluded from analysis (Online Supplemental Data).<sup>27</sup>

### Statistical Analyses

Demographic differences between the nonaerated and control groups were analyzed using a  $\chi^2$  test for categorical variables (sex, ethnicity, maternal education level, handedness); and independent  $t$  tests, for continuous variables (age, nonverbal IQ). Differences in DTI parameters between the nonaerated and control groups were tested using ANCOVA. Covariates were added to the ANCOVA models if they resulted in a  $> 5\%$  change in the effect estimate. Covariates included the child's age at scanning and sex. Results were reported in effect sizes (Cohen's  $d$ ) with  $P$  values. The threshold for significance was set at  $P < .05$ .

Because the control group does include children with minor degrees of mucosal thickening of their sinuses (score 1) and the significance of this minor degree of mucosal thickening is not clear, 2 additional sensitivity analyses were performed assessing different WM tracts: an analysis comparing the 2 extreme categories (score 0 versus 2/3) and an analysis using a classification into 3 groups (score 0 versus 1 versus 2/3).

To account for possible age differences between the nonaerated and control groups seen in our total study population, we performed a subsequent subanalysis in children with nonaerated paranasal sinuses showing a significant effect on mean FA values of specific WM tracts in the ANCOVA. To perform this subanalysis, for each subgroup of nonaerated paranasal sinuses (Online Supplemental Data), we individually matched cases and controls so that the paired age difference was less than 6 months. The number of age-matched controls in each subgroup was identical to the number of children in the accompanying nonaerated group, ie, 54 and 46 controls in, respectively, the right and left nonaerated frontal sinus groups; 16 and 16 controls in, respectively, the right and left nonaerated ethmoid sinus groups; and 13 and 17 controls in, respectively, the right and left nonaerated sphenoid sinus groups (Online Supplemental Data). Because of the small number of cases in the subgroups of the nonaerated group, results were reported in effect sizes (Cohen's  $d$ ) with 95% CIs instead of  $P$  values. Only effect sizes found to exceed the Cohen's convention (1988) for a medium, large, or very large effect are given.<sup>33</sup>

A VBA of FA and MD values of WM microstructure was performed to provide greater spatial detail of the effect of nonaerated-versus-aerated paranasal sinuses. Because in this VBA a large number of voxels were compared simultaneously, the Benjamini-Hochberg FDR correction was applied to all voxels within the FA and MD masks to correct for multiple testing.<sup>32</sup>

All analyses were performed using R statistical and computing software, Version 4.0.1 (<http://www.r-project.org/>) or the scikit-learn module (<https://scikit-learn.org/stable/>) in Python, Version 3.8.2.

## RESULTS

### Sample Characteristics

Sample characteristics are presented in the Table. A total of 109 children were included in the group with nonaeration of  $\geq 1$



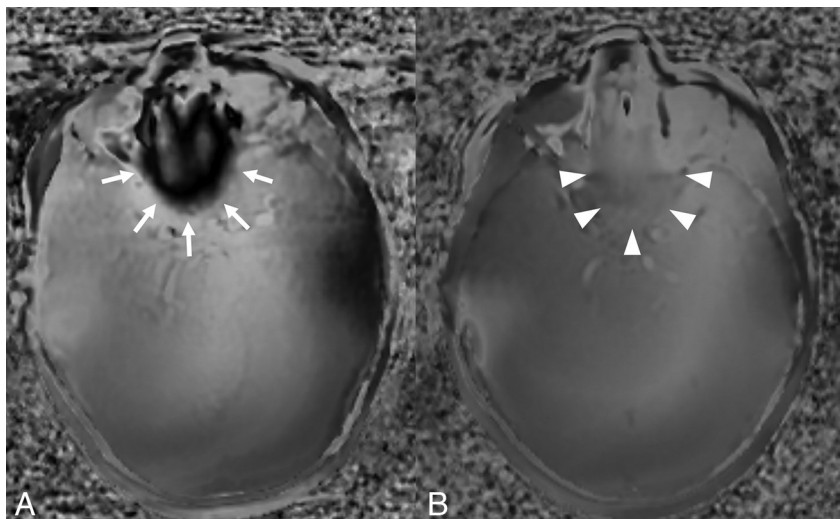


**FIGURE.** DTI phase maps of the brain at the level of ethmoid and sphenoid sinuses. Prominent susceptibility artifacts (arrows) are seen in a participant with well-aerated paranasal sinuses (A). In a participant with nonaerated ethmoid and sphenoid sinuses (B), much fewer susceptibility artifacts are seen (arrowheads).

paranasal sinus, and 110 children were included in the control group. DTI data of 6 and 5 children, respectively, were of insufficient quality and were, therefore, excluded from analysis. Children in the nonaerated sinus and control groups significantly differed in age at the time of scanning ( $t(206) = 2.45, P = .02$ ). There was no difference in sex ( $P = .78$ ), ethnicity ( $P = .37$ ), nonverbal IQ ( $t(171) = 0.97, P = .33$ ), maternal education ( $P = .19$ ), and handedness ( $P = .45$ ) between groups.

### Paranasal Sinuses

The prevalence of neuroimaging signs of mucosal thickening in our cohort was 10.2% (109/1070). The mean modified Lund-Mackay score was 6.56 (SD, 3.60). The Online Supplemental Data show, in more detail, the distribution and degree of nonaerated paranasal sinuses.

DTI phase maps are shown to visualize the distortion (Figure), to demonstrate the effect on magnetic susceptibility caused by well-aerated paranasal sinuses versus nonaerated paranasal sinuses.

### FA and MD Values of Major WM Tracts

The Online Supplemental Data show the differences in mean FA values of major WM tracts between the nonaerated and control groups. Children with nonaerated ethmoid sinuses demonstrated lower mean FA values of the ipsilateral UF (right ethmoid sinus:  $d = -0.03, P = .02$  and left ethmoid sinus:  $d = -0.03, P = .02$ ). Lower mean FA values of the ipsilateral UF were shown in children with nonaerated left sphenoid sinuses ( $d = -0.02, P = .04$ ) and right frontal sinuses ( $d = -0.02, P = .03$ ). The mean FA value of the ipsilateral SLF was lower in children with nonaerated right ethmoid sinuses ( $d = -0.03, P \leq .005$ ), right frontal sinuses ( $d = -0.06, P \leq .005$ ), and right sphenoid sinuses ( $d = -0.04, P \leq .005$ ); there was significant influence of FA values of the ILF in children with nonaerated left frontal sinuses ( $d = -0.02, P = .02$ ). The ipsilateral CGB mean FA value was negatively influenced by the nonaerated left frontal sinus ( $d = -0.02, P = .03$ )

and the right and left sphenoid sinuses (respectively,  $d = -0.04, P \leq .005$ , and  $d = -0.02, P = .04$ ). A lower mean FA value was found in the FMa in children with nonaerated right and left frontal sinuses (respectively,  $d = -0.04, P = .005$ , and  $d = -0.02, P = .03$ ) and the right sphenoid sinuses ( $d = -0.02, P = .04$ ).

The sensitivity analysis of FA values of the major WM tracts in the 3 groups (score 0 versus 1 versus 2/3), and the 2 extreme groups (score 0 versus 2/3) had predominantly similar results. Comparing the 2 extreme groups did show additional lower FA values of the ipsilateral CGB in children with nonaerated right and left ethmoid sinuses as well (respectively,  $d = -0.02, P = .04$ , and  $d = -0.02, P = .03$ ).

In addition, the Online Supplemental Data show the differences in the mean MD values of major WM tracts between the nonaerated and control groups with

the mean MD values of certain major WM tracts demonstrating significant influence caused by nonaerated paranasal sinuses. The mean MD values changed in the opposite direction compared with FA values. Higher mean MD values of the ipsilateral UF were shown in children with nonaerated right and left sphenoid sinuses (respectively,  $d = 0.03, P = .007$ , and  $d = 0.02, P = .04$ ) and nonaerated right frontal sinuses ( $d = 0.02, P = .02$ ). The mean MD value of the ipsilateral SLF was higher in children with nonaerated right frontal sinuses ( $d = 0.02, P = .02$ ), whereas there was no significant influence of MD values of the ILF. A higher mean MD value was found in the FMa in children with nonaerated right and left frontal sinuses (respectively,  $d = 0.05, P \leq .005$ , and  $d = 0.07, P \leq .005$ ) and right and left sphenoid sinuses (respectively,  $d = 0.04, P \leq .005$ , and  $d = 0.02, P = .02$ ).

The subanalysis of the nonaerated paranasal sinuses in which the ANCOVA demonstrated significantly lower mean FA and/or higher mean MD values, using age-matched controls, showed a persistent negative effect on the mean FA values of the UF, SLF, and CGB. The mean FA value of the ipsilateral UF remained lower in children with nonaerated right frontal sinuses ( $n = 24, d = -0.60$ ; 95% CI,  $-0.31$  to  $-1.52$ ). In the ipsilateral SLF, the mean FA value remained lower in children with nonaerated right ethmoid sinuses ( $n = 14, d = -0.56$ ; 95% CI,  $-0.63$  to  $-1.75$ ) and right sphenoid sinuses ( $n = 12, d = -2.09$ ; 95% CI,  $-0.24$  to  $-3.64$ ). The negative effect of nonaerated right sphenoid sinuses ( $n = 12, d = -1.28$ ; 95% CI,  $-0.32$  to  $-2.75$ ) and the left sphenoid sinuses ( $n = 12, d = -1.49$ ; 95% CI,  $-0.19$  to  $-2.94$ ) persisted in the ipsilateral CGB. The results of this subanalysis are shown in the Online Supplemental Data. The mean MD values remained higher only in the FMa in children with nonaerated right and left sphenoid sinuses (respectively,  $n = 12, d = 0.78$ ; 95% CI,  $0.69$ – $2.24$ , and  $n = 12, d = 0.78$ ; 95% CI,  $0.69$ – $2.24$ ).

The proximity of some of the above-mentioned WM tracts to the specific paranasal sinuses is shown in the Online Supplemental data.

## Voxel-Based Analyses

To provide greater spatial detail, we analyzed the effect of nonaerated ethmoid, frontal, and sphenoid sinuses on the FA and MD values of the WM microstructure of the adjacent brain regions using VBA. Overall, the VBA showed focal changes in mean FA and MD values in the WM tracts, consistent with our tract-based approach. The lower FA was localized very focally in the regions of the UF, SLF, and CGB, near the region of the paranasal sinuses. After we performed the FDR correction on all voxels within the FA and MD masks, the VBA showed similar results.

## DISCUSSION

The potential impact of paranasal sinus aeration status and mucosal disease on neuroimaging sequences susceptible to magnetic field inhomogeneity has not been previously reported. DTI is known to be vulnerable to susceptibility artifacts.<sup>5</sup> Most important, analyses of DTI parameters are used increasingly in research projects evaluating typical and atypical brain development in children and adolescents. Our study results show that the amount of air in the paranasal sinuses in close proximity to brain tissue influences the measurements of diffusion characteristics of adjacent WM. The highly regional effect of this impact is further supported by the results of the VBA. This outcome is likely caused by changes in susceptibility directly resulting from different amounts of air that are near the WM tracts of interest.

Previous studies have demonstrated that susceptibility effects can lead to misinterpretation of DTI parameters of the involved brain tissue.<sup>34-36</sup> At tissue-air interface, susceptibility values demonstrate more variation, leading to diminished quality of the local magnetic field and creating field inhomogeneities. The frequency shift in *k*-space results in a spatial shift of voxel intensity and thus images deviating from true brain anatomy.<sup>37-39</sup> If the shifted voxel is still within the volume of the calculated WM tract, there will be less effect on the mean FA value. We focused on major WM tracts, and some of the susceptibility effects from the DTI acquisition seen on the voxel level may have had less influence on the level of a WM tract. Tract-based DTI analyses are the workhorse in the current published studies investigating the microstructure of the pediatric brain.<sup>1-4</sup> We think that only focusing on voxel-based FA and MD would ignore the common practice in this research field. This study shows that the amount of air in the paranasal sinuses affects FA and MD values of the WM in close proximity to those sinuses and also translates into the effects on mean FA and MD values of some of the major WM tracts. Susceptibility distortions can potentially be diminished using geometric corrections of the structural image, estimate maps of  $B_0$  inhomogeneities acquired using gradient-echo scans, and estimates of the underlying distortions derived from additional data acquired using reversed phase-encoding.

Typically, FA and MD change in opposite directions; however, susceptibility effects can change them in a similar manner.<sup>40,41</sup> Because FA reflects directionality in diffusion, there is a more direct relation to WM microarchitecture, in contrast to MD.<sup>42,43</sup> Our results illustrate less influence of aerated-versus-nonaerated paranasal sinuses on mean MD values of major WM tracts than on FA values. MD values by themselves are nonspecific, however, and should be used in conjunction with other diffusion

tensor parameters.<sup>44</sup> The lower FA values in the nonaerated group likely better reflect the true underlying values because nonaerated sinuses lead to fewer susceptibility-related distortions. This reasoning is in line with previous studies showing that susceptibility distortion-correction methods cause reductions in whole-brain WM FA values and corresponding higher MD values.<sup>37,45</sup>

This study demonstrates the relevance of considering the extent of mucosal thickening or the degree of pneumatization of the paranasal sinuses in the region of the skull base (ie, as a covariate or using it in sensitivity analyses) before interpreting DTI parameters of the brain, especially in pediatric populations. In studies focusing on typical development of the pediatric brain, changes in DTI parameters of specific WM tracts, such as the ILF, UF, and CGB, are described.<sup>14</sup> Knowledge of potential factors that can modify the signal, such as nonaerated paranasal sinuses, is especially relevant when the study population includes a relative large sample of children between 3 and 8 years of age (peak age of inflammatory paranasal sinus disease<sup>7,8</sup>). In addition, because some neurodevelopmental disorders may increase the risk of sinusitis (eg, craniofacial syndromes, neuromuscular disorders),<sup>46,47</sup> it is important to incorporate knowledge of the potential effect of the degree of aeration of paranasal sinuses on DTI parameters in these study designs. Because we excluded the maxillary sinus from our analyses (due to the relatively large separation between the maxillary sinus and the anterior-inferior brain regions), we did not assess the potential effects of nonaerated maxillary sinuses on measurements of WM diffusion characteristics. This assessment could be an interesting focus for future research.

There are a number of strengths of the population-based study, including standardized DTI measurements obtained in a large sample derived from the general pediatric population. However, there are also limitations. We were unable to determine a distortion-correction factor due to the small number of children with completely nonaerated paranasal sinuses. In addition, the younger children did show more mucosal thickening and less pneumatization of the paranasal sinuses. Although we tried to take age differences into account, we cannot completely exclude residual confounding. Additionally, DTI phase maps (instead of field maps) were acquired in the study protocol. The lack of acquired field maps is a limitation of the study because we were able to create distortion maps to further illustrate the effect of air/nonaeration. To minimize the effect of geometric distortion, we applied a nonlinear registration of the FA maps to a study-specific EPI template in standard space, a method favoring other distortion-correction methods as shown in the literature.<sup>31</sup>

## CONCLUSIONS

Nonaeration of the paranasal sinuses is a common incidental finding on MR imaging of the pediatric brain. We demonstrate that the amount of mucosal thickening or the degree of pneumatization of the paranasal sinuses influences FA and, to a lesser degree, MD values of major WM tracts close to the skull base region in 6- to 9-year-old children.

Disclosure forms provided by the authors are available with the full text and PDF of this article at [www.ajnr.org](http://www.ajnr.org).

## REFERENCES

- López-Vicente M, Lamballais S, Louwen S, et al. **White matter microstructure correlates of age, sex, handedness and motor ability in a population-based sample of 3031 school-age children.** *Neuroimage* 2021;227:117643 [CrossRef Medline](#)
- Lebel C, Walker L, Leemans A, et al. **Microstructural maturation of the human brain from childhood to adulthood.** *Neuroimage* 2008;40:1044–55 [CrossRef Medline](#)
- Schmithorst VJ, Yuan W. **White matter development during adolescence as shown by diffusion MRI.** *Brain Cogn* 2010;72:16–25 [CrossRef Medline](#)
- Giorgio A, Watkins KE, Chadwick M, et al. **Longitudinal changes in grey and white matter during adolescence.** *Neuroimage* 2010;49:94–103 [CrossRef Medline](#)
- Atlas SW, ed. **Magnetic resonance imaging of the brain and spine.** Vol. 1. Lippincott Williams & Wilkins; 2009
- Tax CM, Vos SB, Leemans A. **Checking and Correcting DTI Data.** In: Van Hecke W, Emsel L, Sunaert S, eds. *Diffusion Tensor Imaging*. Springer-Verlag; 2016:127–50
- von Kalle T, Fabig-Moritz C, Heumann H, et al. **Incidental findings in paranasal sinuses and mastoid cells: a cross-sectional magnetic resonance imaging (MRI) study in a pediatric radiology department.** *Rofo* 2012;184:629–34 [CrossRef Medline](#)
- Gordts F, Clement PA, Destryker A. **Prevalence of sinusitis signs on MRI in a non-ENT pediatric population.** *Rhinology* 1997;35:154–57 [Medline](#)
- Jansen PR, Dremmen M, van den Berg A, et al. **Incidental findings on brain imaging in the general pediatric population.** *N Engl J Med* 2017;377:1593–95 [CrossRef Medline](#)
- Kim BS, Illes J, Kaplan RT. **Incidental findings on pediatric MR images of the brain.** *AJNR Am J Neuroradiol* 2002;23:1674–77 [Medline](#)
- Lim WK, Ram B, Fasulakis S, et al. **Incidental magnetic resonance image sinus abnormalities in asymptomatic Australian children.** *J Laryngol Otol* 2003;117:969–72 [CrossRef Medline](#)
- Scuderi AJ, Harnsberger HR, Boyer RS. **Pneumatization of the paranasal sinuses: normal features of importance to the accurate interpretation of CT scans and MR images.** *AJR Am J Roentgenol* 1993;160:1101–04 [CrossRef Medline](#)
- Adibelli ZH, Songu M, Adibelli H. **Paranasal sinus development in children: a magnetic resonance imaging analysis.** *Am J Rhinol Allergy* 2011;25:30–35 [CrossRef Medline](#)
- Krogsrud SK, Fjell AM, Tamnes CK, et al. **Changes in white matter microstructure in the developing brain: a longitudinal diffusion tensor imaging study of children from 4 to 11 years of age.** *Neuroimage* 2016;124:473–86 [CrossRef Medline](#)
- Mukherjee P, Miller JH, Shimony JS, et al. **Normal brain maturation during childhood: developmental trends characterized with diffusion-tensor MR imaging.** *Radiology* 2001;221:349–58 [CrossRef Medline](#)
- Jaddoe VW, Mackenbach JP, Moll HA, et al. **The Generation R Study: design and cohort profile.** *Eur J Epidemiol* 2006;21:475–84 [CrossRef Medline](#)
- White T, Muetzel RL, El Marroun H, et al. **Paediatric population neuroimaging and the Generation R Study: the second wave.** *Eur J Epidemiol* 2018;33:99–125 [CrossRef Medline](#)
- Basten M, van der Ende J, Tiemeier H, et al. **Nonverbal intelligence in young children with dysregulation: the Generation R Study.** *Eur Child Adolesc Psychiatry* 2014;23:1061–70 [CrossRef Medline](#)
- Oldfield RC. **The assessment and analysis of handedness: the Edinburgh inventory.** *Neuropsychologia* 1971;9:97–113 [CrossRef Medline](#)
- White T, El Marroun H, Nijs I, et al. **Pediatric population-based neuroimaging and the Generation R Study: the intersection of developmental neuroscience and epidemiology.** *Eur J Epidemiol* 2013;28:99–111 [CrossRef Medline](#)
- Lund VJ, Kennedy DW. **Staging for rhinosinusitis.** *Otolaryngol Head Neck Surg* 1997;117:S35–40 [CrossRef](#)
- Lin HW, Bhattacharyya N. **Diagnostic and staging accuracy of magnetic resonance imaging for the assessment of sinonasal disease.** *Am J Rhinol Allergy* 2009;23:36–39 [CrossRef Medline](#)
- Yousefi F, Mollabashi M, Shokri A, et al. **Magnetic resonance imaging study of incidental findings in the paranasal sinuses and ostiomeatal complex.** *Imaging Sci Dent* 2022;52:11–18 [CrossRef Medline](#)
- Smith SM, Jenkinson M, Woolrich MW, et al. **Advances in functional and structural MR image analysis and implementation as FSL.** *Neuroimage* 2004;23(Suppl 1):S208–19 [CrossRef Medline](#)
- Andersson JL, Sotiropoulos SN. **An integrated approach to correction for off-resonance effects and subject movement in diffusion MR imaging.** *Neuroimage* 2016;125:1063–78 [CrossRef Medline](#)
- Mulder TA, Kocenska D, Muetzel RL, et al. **Childhood sleep disturbances and white matter microstructure in preadolescence.** *J Child Psychol Psychiatry* 2019;60:1242–50 [CrossRef Medline](#)
- Muetzel RL, Mous SE, van der Ende J, et al. **White matter integrity and cognitive performance in school-age children: a population-based neuroimaging study.** *Neuroimage* 2015;119:119–28 [CrossRef Medline](#)
- de Groot M, Vernooij MW, Klein S, et al. **Improving alignment in tract-based spatial statistics: evaluation and optimization of image registration.** *Neuroimage* 2013;76:400–11 [CrossRef Medline](#)
- Dall'Aglia L, Xu B, Tiemeier H, et al. **Longitudinal associations between white matter microstructure and psychiatric symptoms in adolescence.** *medRxiv* 22279298;2022. <https://www.medrxiv.org/content/10.1101/2022.08.27.22279298v1>. Accessed September 30, 2022
- Luque Laguna PA, Combes AJE, Streffer J, et al. **Reproducibility, reliability and variability of FA and MD in the older healthy population: a test-retest multiparametric analysis.** *Neuroimage Clin* 2020;26:102168 [CrossRef Medline](#)
- Calhoun VD, Wager TD, Krishnan A, et al. **The impact of T1 versus EPI spatial normalization templates for fMRI data analyses.** *Hum Brain Mapp* 2017;38:5331–42 [CrossRef Medline](#)
- Benjamini Y, Hochberg Y. **Controlling the false discovery rate: a practical and powerful approach to multiple testing.** *J R Stat Soc* 1995;57:289–300 [CrossRef](#)
- Cohen J. *Statistical Power Analysis for the Behavioral Sciences.* Academic press, 2013
- Hiwatashi A, Kinoshita T, Moritani T, et al. **Hypointensity on diffusion-weighted MRI of the brain related to T2 shortening and susceptibility effects.** *AJR Am J Roentgenol* 2003;181:1705–09 [CrossRef Medline](#)
- Haris M, Gupta RK, Husain N, et al. **Measurement of DTI metrics in hemorrhagic brain lesions: possible implication in MRI interpretation.** *J Magn Reson Imaging* 2006;24:1259–68 [CrossRef Medline](#)
- Pfefferbaum A, Adalsteinsson E, Rohlfing T, et al. **Diffusion tensor imaging of deep gray matter brain structures: effects of age and iron concentration.** *Neurobiol Aging* 2010;31:482–93 [CrossRef Medline](#)
- Lahti K, Parkkola R, Jääsaari P, et al; PIPARI Study Group. **The impact of susceptibility correction on diffusion metrics in adolescents.** *Pediatr Radiol* 2021;51:1471–80 [CrossRef Medline](#)
- Huang H, Ceritoglu C, Li X, et al. **Correction of B0 susceptibility induced distortion in diffusion-weighted images using large-deformation diffeomorphic metric mapping.** *Magn Reson Imaging* 2008;26:1294–302 [CrossRef Medline](#)
- Embleton KV, Haroon HA, Morris DM, et al. **Distortion correction for diffusion-weighted MRI tractography and fMRI in the temporal lobes.** *Hum Brain Mapp* 2010;31:1570–87 [CrossRef Medline](#)
- Lebel C, Gee M, Camicioli R, et al. **Diffusion tensor imaging of white matter tract evolution over the lifespan.** *Neuroimage* 2012;60:340–52 [CrossRef Medline](#)
- Schmithorst VJ, Wilke M, Dardzinski BJ, et al. **Correlation of white matter diffusivity and anisotropy with age during childhood and adolescence: a cross-sectional diffusion-tensor MR imaging study.** *Radiology* 2002;222:212–18 [CrossRef Medline](#)

42. Mukherjee P, Berman JI, Chung SW, et al. **Diffusion tensor MR imaging and fiber tractography: theoretic underpinnings.** *AJNR Am J Neuroradiol* 2008;29:632–41 [CrossRef Medline](#)
43. Mukherjee P, Chung SW, Berman JI, et al. **Diffusion tensor MR imaging and fiber tractography: technical considerations.** *AJNR Am J Neuroradiol* 2008;29:843–52 [CrossRef Medline](#)
44. Sijens PE, Irwan R, Potze JH, et al. **Relationships between brain water content and diffusion tensor imaging parameters (apparent diffusion coefficient and fractional anisotropy) in multiple sclerosis.** *Eur Radiol* 2006;16:898–904 [CrossRef Medline](#)
45. Irfanoglu MO, Sarlls J, Nayak A, et al. **Evaluating corrections for eddy-currents and other EPI distortions in diffusion MRI: methodology and a dataset for benchmarking.** *Magn Reson Med* 2019;81:2774–87 [CrossRef Medline](#)
46. Leo G, Triulzi F, Incorvaia C. **Diagnosis of chronic rhinosinusitis.** *Pediatr Allergy Immunol* 2012;23(Suppl 22):20–26 [CrossRef Medline](#)
47. Heath J, Hartzell L, Putt C, et al. **Chronic rhinosinusitis in children: pathophysiology, evaluation, and medical management.** *Curr Allergy Asthma Rep* 2018;18:37 [CrossRef Medline](#)